Thermodynamic Modeling of Alterations During Climate Transition Reveals Evidence of Past Temperate Conditions on Venus

H. T. White[1,2] and V. F. Chevrier[1]

[1]Arkansas Center for Space and Planetary Sciences, University of Arkansas, Fayetteville, AR 72701, USA.

[2]Department of Earth and Space Sciences, University of Washington, Seattle, WA 98195, USA.

Corresponding author: Haskelle White (hasktw@uw.edu)

Key Points:

- We show that the interaction between the venusian crust, atmosphere, and paleo-ocean can reproduce the present-day atmosphere of Venus.
- The evolution of various atmospheric gases is consistent with rising surface temperatures.
- Our model's resulting mineral parageneses may be indicative of past temperate conditions.

Abstract

We modeled the thermodynamic evolution of the venusian crust in the presence of an atmosphere and paleo-ocean during a potential climate transition to its present uninhabitable state. We show that the present-day atmospheric composition of Venus is reproduced by the interaction between a paleo-ocean and crust during a runaway greenhouse. The evolution of oxygen fugacity with increasing surface temperatures converges with the present-day value (10^{-20} bar) at current temperatures (400-500°C). Other atmospheric species (CO, CH_4, H_2S, SO_2) show varying behavior depending on RedOx, but are consistent with increasing oxygen fugacity. Low-pressure conditions result in the genesis of unique mineral parageneses, including tremolite and zeolites, that could survive on Venus over geological timescales and are indicative of stable liquid water in the past if detected by future missions. Therefore, the resulting venusian mineralogy in our models could be markers of past habitable conditions that were altered by a significant greenhouse effect.

Plain Language Summary

The possibility of habitable conditions with abundant liquid water and cooler temperatures in the history of Venus remains a long-standing question in the exploration of Earth's twin sister. Studying Venus' transition to its present uninhabitable state is critical to understanding terrestrial planet evolution and whether these planets can become habitable. However, how this transition occurred is not well understood, as Venus' thick atmosphere and recent volcanic activity obscures the planet's surface. Here, we use a mathematical model that calculates the chemical reactions between the venusian crust, atmosphere, and paleo-ocean. Our model demonstrates that the interaction between Venus' crust and paleo-ocean can reproduce the present-day atmosphere. These interactions also produced unique minerals that could be evidence of past temperate climates and stable liquid water if detected by future missions. We show that present-day Venus conditions could have resulted from a past habitable climate that experienced increasing temperatures induced by a potential climate transition.

Keywords: *Venus, Climate Transition, Thermodynamic Modeling, Paleoclimate, Habitability*

1 Introduction

Venus is the hottest planet in our solar system, with surface pressures and temperatures unsuitable for life. However, early in the Solar System's history, when the Sun was 30% dimmer, Venus resided comfortably in the Sun's habitable zone (Kasting, 1993; Kopparapu et al., 2013). Venus' favorable location and the similarities between Earth's and Venus' global compositions have caused many to speculate whether Venus was once habitable. Several models demonstrated that Venus could have maintained habitable temperatures and pressures for much of its history (Kasting, 1988; Way & Del Genio, 2020; Krissansen-Totton et al., 2021). Evidence for stable liquid water from elevated D/H ratios also supported early habitability, implying a shallow reservoir in the past that was progressively lost to space through hydrogen escape (Donahue & Russell, 1997; De Bergh et al., 2006).

Studies of the planet's surface composition, interactions with the atmosphere, and geophysical processes in the interior have revealed about the surface mineralogy. Although

surface mineralogy has never been directly analyzed, *in situ* X-ray fluorescence and gamma-ray spectroscopy from Venera landers have acquired the elemental compositions of some locations (Surkov et al., 1984), from which modal abundances were derived. Previous thermodynamic models and theoretical calculations have shown that some hydrous minerals might remain stable under Venus's current surface conditions (Zolotov et al., 1997; Semprich et al., 2020). However, little research has been done to examine the effect of a runaway greenhouse on the composition of the various surface reservoirs (atmosphere, crust, and hydrosphere). This work presents the results of a global thermodynamic model of Venus' geochemical evolution during a major climate transition from temperate (terrestrial-like pressure and temperature) to present-day Venusian (average P, T = 95 bar, 460ºC).

2 Methods: Geochemical Modeling

To model the geochemical evolution of Venus, we use the *Geochemist's Workbench 17*® software, specifically the *React* module, to simulate the equilibrium parageneses between various crust models, a primitive ocean, and the atmosphere as a function of temperature. We used three different models of crust: a tholeiitic basalt based on Venera 13's in situ measurements of the surface (Surkov et al., 1984), and two models of ancient terrains, the so-called tesserae: a granodiorite and an anorthosite, based on emissivity observations (Gilmore et al., 2015). We used standard terrestrial seawater as an ocean composition (Alanezi & Hilal, 2007). For the atmosphere, we used two CO_2 surface pressures: 1 bar to represent an ancient terrestrial "habitable" Venus and 100 bar to replicate current surface conditions. RedOx potential is not fixed in the model as there is no constraint on oxygen fugacity (fO_2) in the atmosphere of Venus. Instead, we consider global crust-ocean interaction that would buffer the atmosphere and the resulting fO_2 evolution. Initial oxidizing conditions are set to pE = 13.05 based on the iron RedOx couple (Fe^{2+}/Fe^{3+}, e.g. Chevrier & Morrison, 2020) that is prevalent on the surface of Venus. We then simulated the evolution of equilibrium parageneses as a function of temperature between 25 and 300°C (the highest temperature achievable by the thermodynamic database). For more information on the model's parameters and how to run it, see the Supporting Information and refer to White (2024).

3 Results

Overall, the alteration of our three models of primary crust results in globally similar mineral parageneses and a variety of phases as a function of temperature (Fig. 1). Table S1 in the Supporting Information section provides an exhaustive list of the minerals present in the results, along with their composition. Quartz is the most abundant phase at high pressure, while quartz, dolomite, mesolite, calcite, and corundum (in order of increasing temperature) are the dominant phases at low pressure. However, quartz is the dominant phase in both pressure models of granodiorite. At low pCO_2, we observe roughly three regions for mineral assemblages as a function of temperature: below 100°C, between 100 and 200°C, and above 200°C. At higher pCO_2, we only observe two regions, with a transition around 150°C. Low temperatures (< 100°C) show similar assemblages at both low and high pressures, composed of quartz, carbonates, phyllosilicates, and diaspore. At low pressure, the intermediate temperature (100-200°C) paragenesis is quite complex but is essentially composed of zeolite (mesolite), phyllosilicates (smectites and micas), and feldspar. At high temperatures, noticeable mineralogical differences are observed between the low- and high-pressure simulations. Some

phases are common to both pressures, such as corundum, microcline, and saponite-Na. However, several high-temperature silicates only appear at low pressure, including tremolite, diopside, tephroite, and andradite.

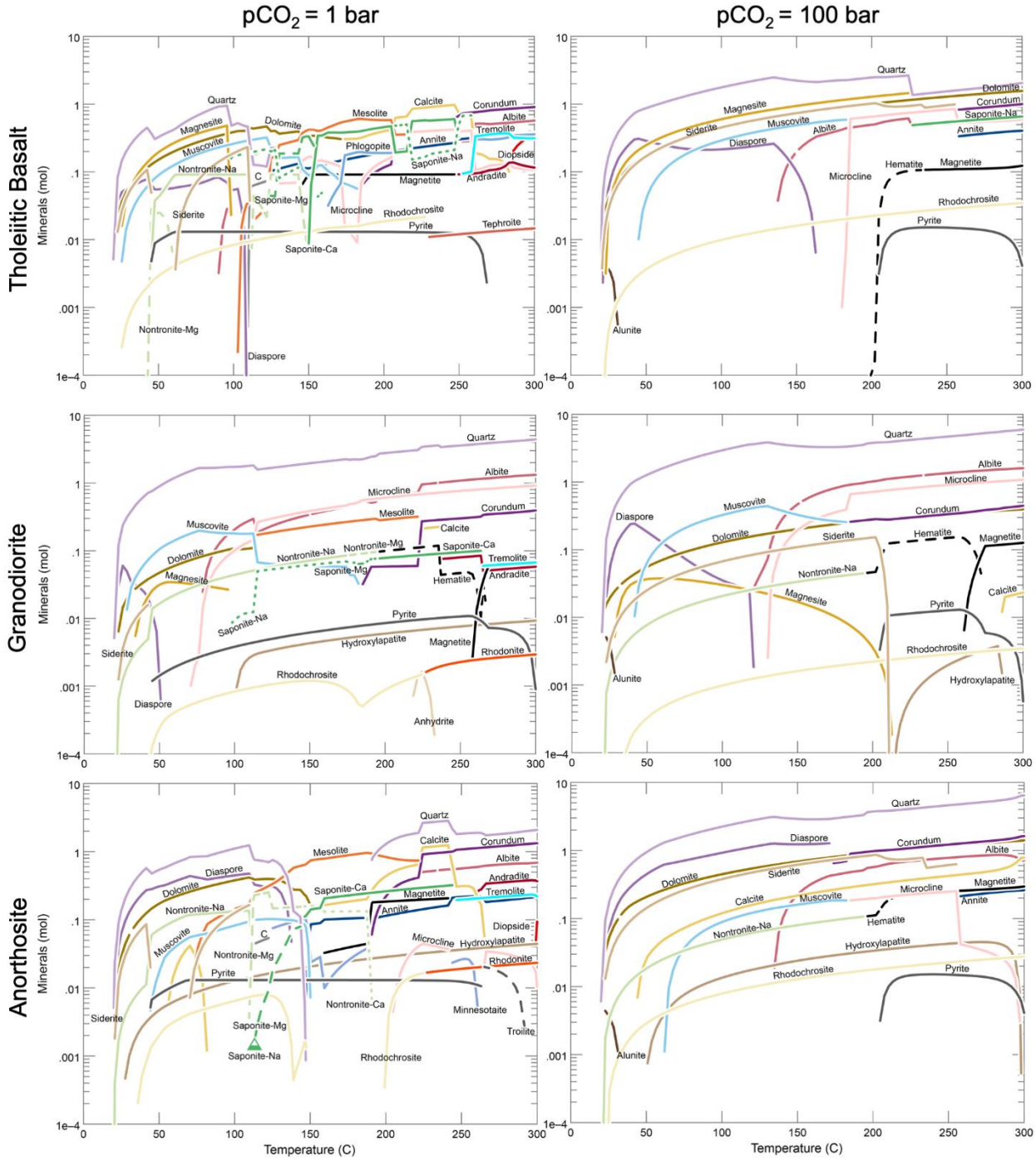

Figure 1: Evolution of mineral assemblages as a function of temperature for tholeiitic basalt (Surkov et al., 1984), granodiorite tessera (Hu et al., 2014), and gabbroic anorthosite tessera (Mukherjee et al., 2005) under initial oxidizing conditions (pE = 13.05). Lines denote a specific mineral's evolution that result from the interaction of the crust with the paleo-ocean and atmosphere. Dashed and dotted lines differentiate minerals with similar chemical formulas.

Mineral groups and sub-groups are divided by similar color shades: Nesosilicates, Pyroxenoids = red; Zeolites = orange; Carbonates = yellow; Smectites = green; Micas, Talc, Amphiboles = Blue; Aluminum and Silica Oxides = purple, Feldspars = pink; Sulfates, Phosphates = Brown. Sulfides, Native Elements = gray; Iron Oxides = black.

Regarding iron-bearing minerals, low-temperature, and low-pressure conditions show siderite and various nontronites. At high temperatures, nontronite typically destabilizes into iron oxide magnetite and, finally, into andradite garnet. At high pressure, nontronite destabilizes into iron oxides hematite, then magnetite. At low pressure, the iron sulfide pyrite is stable at most temperatures, but at high pressure, it only appears at high temperatures.

4 Discussion

In addition to the mineralogical transformation of the crust, the atmospheric composition also undergoes significant changes with increasing temperature. The most important parameter controlling atmospheric composition is the fugacity of oxygen (fO_2), which was calculated by our model as a function of temperature. Each model's fO_2 significantly increases with temperature from 10^{-60} bar at 25ºC to 10^{-30} bar at 300ºC (Fig. 2). There is also no significant variation of fO_2 between the three models we tested (Fig. 2). fO_2 values typically spread over five orders of magnitude, which is relatively small compared to the 30 orders of magnitude change of fO_2 over the entire modelled temperature range. Carbon species buffer the atmospheric fO_2 of Venus since CO_2 constitutes 96% of the atmosphere (Oyama et al., 1980). Sulfur species could only contribute to a small fraction of the atmospheric fO_2. Therefore, the fO_2 is probably the least susceptible to fluctuations, as shown by the limited variability of our fO_2 modelled data (Fig. 2). Although our simulations do not extend beyond 300°C, the resulting fO_2 likely follows a steady trend because the mineral parageneses remain unchanged at higher temperatures (being dominated by anhydrous silicates or oxides similar to what would be present in a rock crystallized at high temperature). In those conditions, the fO_2 values depend on temperature rather than redox equilibria. At temperatures above 300°C, the paleo-ocean was most likely completely vaporized into the atmosphere. The water would be in a supercritical state but continue to react with the surface; thus, oxidation would continue, and fO_2 would keep rising (Zheng et al., 2020). Therefore, the fugacity data for each model were extrapolated via simple exponential fit up to the present-day value of $fO_2 \sim 10^{-20}$ (Fegley et al., 1997). All the resulting equilibrium temperatures are comprised between 400 and 500°C, which is very close to Venus' main surface temperature of 465°C. The 1 bar basalt, 100 bar granodiorite, and 1 bar anorthosite models show the most accurate predictions.

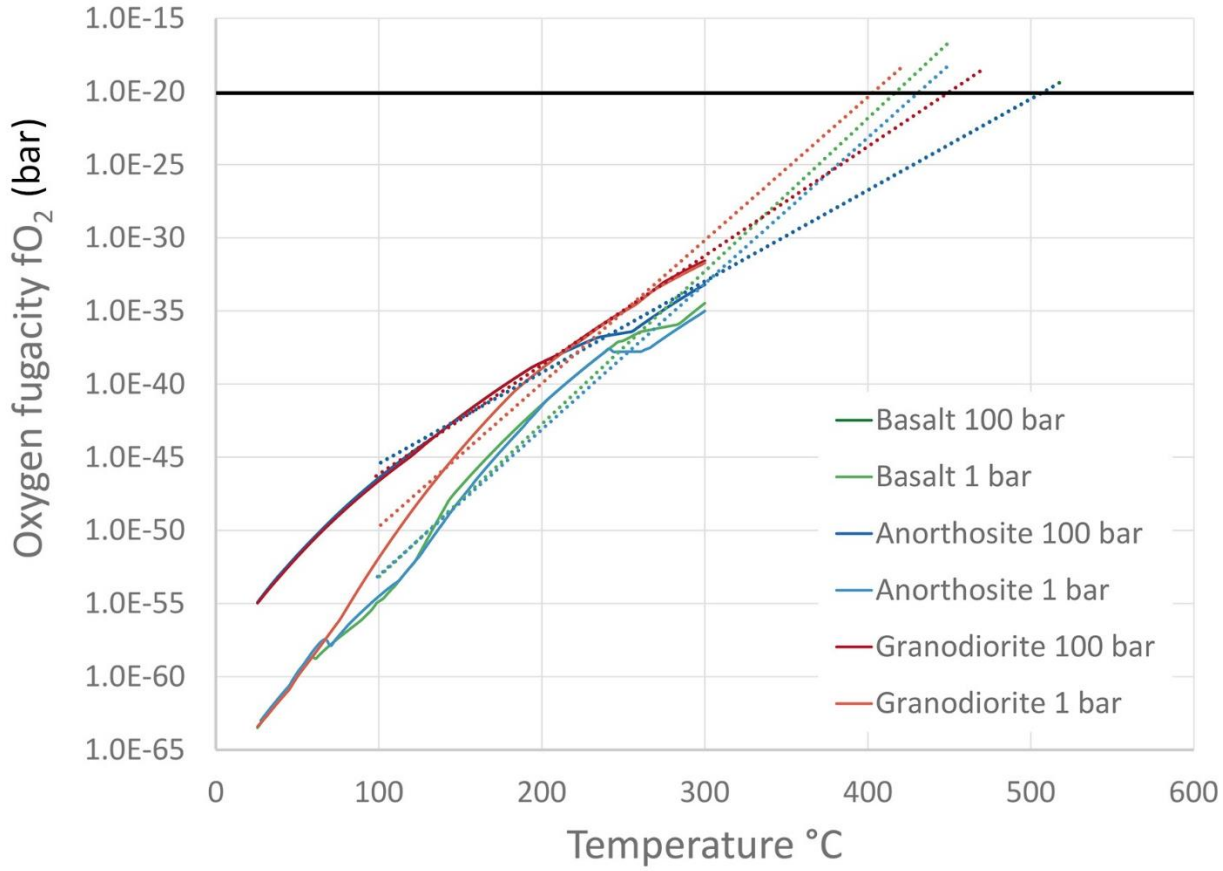

Figure 2: Oxygen fugacity (fO_2) of the system. The plot combines results from each crustal model under oxidizing conditions at high and low pressure, which are denoted by different colored lines. Colors are grouped by crustal model. The 100 bar anorthosite and basalt models produce very similar gas fugacities, as a result, their lines are identical. The black line is the predicted fO_2 at current Venus temperatures calculated from CO observations by Pioneer and Venera spacecraft (Fegley et al., 1997), but we plot it at all temperatures. Dotted lines denote the extrapolation of each model.

We also determined the evolution of various important gas fugacities in the atmosphere of Venus: methane CH_4, carbon monoxide CO, hydrogen sulfide H_2S and sulfur dioxide SO_2 (Fig. 3). All four species' fugacities increase with temperature but not necessarily monotonously. Nonetheless, as a test of our fO_2 extrapolation, we also extrapolated the gas fugacities based on the data in the range 100-300ºC to their present-day measured value. The fugacity of reduced species (CH_4 and H_2S) tends to increase faster with temperature compared to oxidized species (SO_2 and CO). Reduced species show low equilibrium temperatures at present-day atmospheric fugacities, e.g., 100-300ºC for CH_4 and 150-200ºC for H_2S. Therefore, these low values indicate that these species are currently undersaturated compared to equilibrium fugacity values. On the other hand, oxidized species (CO, SO_2) show higher equilibrium temperatures between 300 and 450ºC for CO and between 400 and 600ºC for SO_2, in both cases quite close to the mean Venusian surface temperatures. Moreover, the fugacity of reduced species is strongly affected by

the pressure of CO_2, where both CH_4 and H_2S have fugacities at 1 bar of CO_2 that are 1015 orders of magnitude above the values at 100 bar, but only for temperatures below 100ºC. The fugacity values for both pressures converge with increasing temperature. The fugacity values of CH_4 converges to the present atmospheric concentration of 980 ppm (Donahue & Hoffman, 1993) typically from 250-300°C. The 1 bar granodiorite converges at 660°C (Fig. 3A), although the low p_{CO2} CH_4 fugacities seem to plateau and reach a maximum value above 100ºC. In all low-pressure models, CO fugacity values increase sharply below 100ºC but then exhibits a decrease in fO_2 increase rate above (Fig. 3B). The 1 bar models converge with the present-day concentration of 28 ppm at 350-450ºC, which is closer to Venus' current surface temperatures compared to the 100 bar model predictions which converge around 300ºC (Hoffman et al., 1980a). H_2S is interesting as it shows no variation of fugacity with the nature of the crust but extreme differences with CO_2 pressure (Fig. 3C). Akin to CH_4, H_2S fugacity values at p_{CO2} = 100 bar are 10 to 15 orders of magnitude lower than their 1 bar counterpart, but all values converge to the present day H_2S atmospheric abundance of 3 ppm (Hoffman et al., 1980b) at temperatures around 200°C. Finally, the evolution of SO_2's fugacity differs depending on the nature of the crust (Fig. 3D). Basalt and anorthosite's SO_2 fugacity peaks from 200-300°C while granodiorite consistently increases. The 1 bar models show significant fluctuations at 100°C and 300°C, while the 100 bar models and granodiorite model show a rapid and monotonous increase. These fluctuations result in a higher variability in the final equilibrium temperatures, which are nonetheless in the range 400-600°C for an average SO_2 surface concentrations of 25 ppm (Bézard et al., 1993).

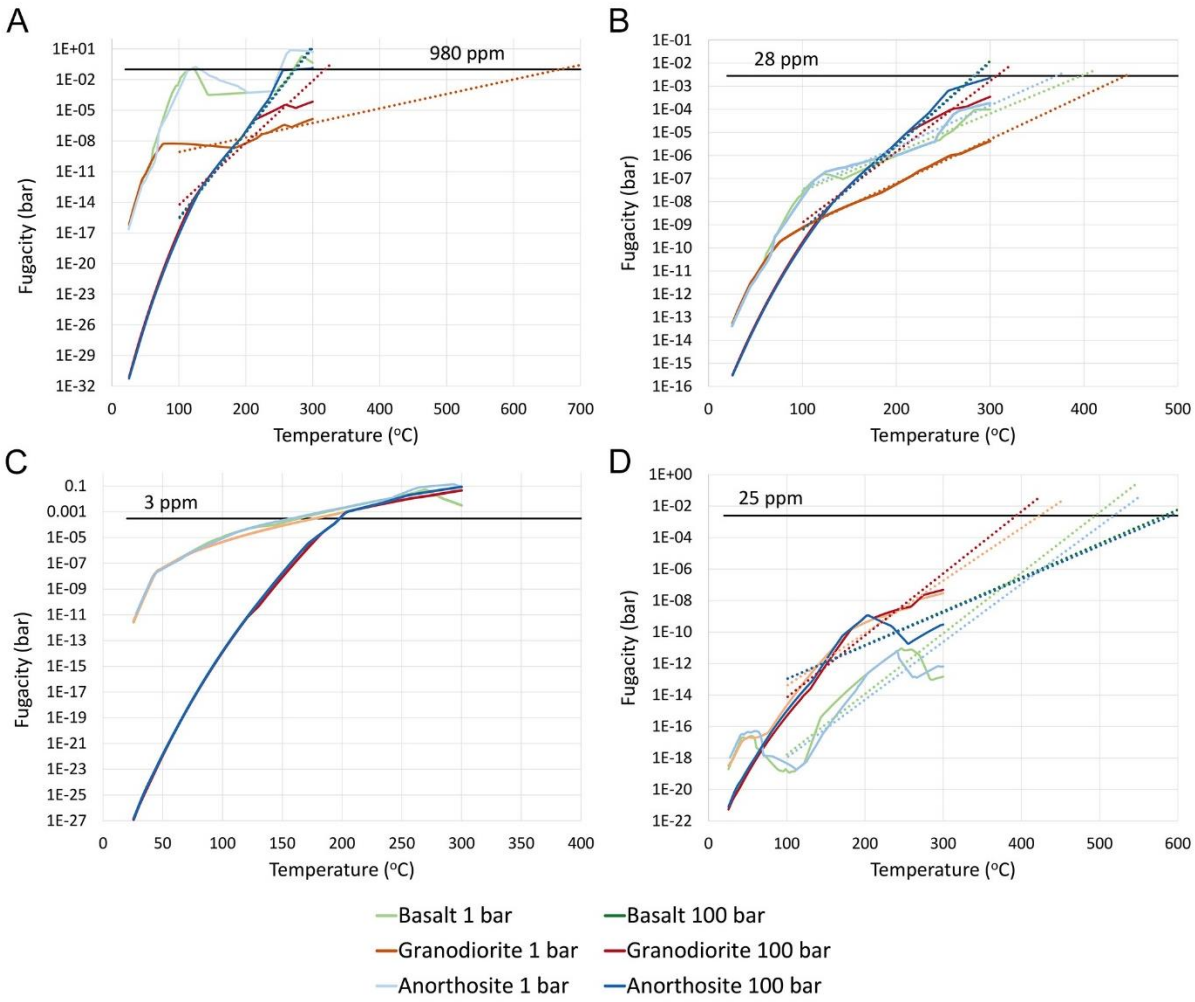

186

187 **Figure 3:** Fugacity of CH_4 (A), CO (B), H_2S (C), and SO_2 (D) under different partial pressures of
188 CO_2 for each crust model (all models have initial oxidizing conditions). Plots use the same color
189 key as Figure 2. Some trendlines are omitted if the model converges with modern-day
190 observations. Black lines are the predicted present-day values based on spectroscopic
191 observations, and have only been observed at present Venus temperatures (~465°C) but we show
192 them across a wide temperature range (Donahue & Hodges, 1993; Hoffman et al., 1980a;
193 Hoffman et al., 1980b; Bézard et al., 1993).

194

195 The difference in behavior between reduced and oxidized species and the respective low
196 versus high temperatures reached at equilibrium with present-day atmospheric abundances are
197 essentially due to oxygen fugacity. Our extrapolations do not consider the effect of increasing
198 fO_2 on the abundance of reduced gas. It is highly likely that the fugacity of these gases would not
199 significantly increase at high fO_2, as shown by the significant drop in rate for the fugacity of H_2S
200 above 50ºC for low pressure or 200ºC for high pressure. The same observation can be made for
201 CH4 which plateaus at temperatures around 100ºC in low p_{CO2} simulations. Thus, CH_4's and
202 H_2S's fugacity slopes become significantly shallower at high temperatures and could result in

higher equilibrium temperatures compared to our extrapolations, although if those species are indeed significantly undersaturated, this could also indicate an active source for those reduced gas species such as volcanism (Herrick and Hensley, 2023).

Our model focuses on equilibria in the presence of liquid water. However, other mechanisms could affect the concentrations of compounds in the atmosphere. Photochemistry in the upper cloud layer (60-70 km) oxidizes SO_2 into H_2SO_4 (Yung & Demore, 1982; Krasnopolsky, 2007), creating a continuous sink for SO_2. In fact, the entire sulfur cycle could modify the atmospheric abundances resulting from surface alteration. Other sinks for sulfur and carbon species could be related to reactions with surface minerals. For example, the abundance of sulfur compounds could be affected by the formation of sulfides (pyrite in our model; Kohler, 2016) or sulfates (anhydrite; Zolotov, 2007). On the other hand, recent observations of active volcanism on Venus could provide sources for these gases (Filiberto et al., 2020; Herrick & Hensley, 2023). Those processes would systematically affect the equilibrium fugacities.

5 Conclusions

In the absence of any in situ identification of secondary phases, the mineralogical results presented in this study remain hypothetical. However, considering the strong arguments made by the atmospheric components and the oxygen fugacity, we can conclude that some specific phases that could survive geological timescales on the Venusian surface could be indicators of past environments. Most hydrated phases that precipitate at low temperatures would most likely not survive. However, phases like tremolite, a water-carrying amphibole, have been shown to remain stable in the current Venusian surface conditions but are characteristic of high temperatures and low CO_2 pressure. Mesolite (a zeolite) is a consistent tracer of intermediate temperatures and low CO_2 pressures. The detection of these phases by future spacecraft or landers/rovers would indicate a past environment with stable liquid water, lower pressures, and lower temperatures. This model does not reach current Venus's temperatures; consequently, some minerals (e.g., hydroxides) may destabilize in modern Venus conditions. However, our model predictions of gas and especially oxygen fugacities reproduced present-day observations and models. Therefore, we show that the current Venusian surface environment results from past habitable conditions that were altered by a significant greenhouse effect that increased temperatures and pressures. Modeling the atmospheric and mineralogical parageneses resulting from this transition helps constrain past conditions on the Venusian surface and identify signs of habitability on terrestrial planets and exoplanets.

Acknowledgments

This work was supported by the Summer Undergraduate Program for Planetary Research (SUPPR) and the LPI Cooperative Agreement. This material is based upon work supported by the NSF Graduate Research Fellowship under Grant No. DGE-2140004.

Open Research

The dataset containing the thermodynamic calculations used in this research is the thermo.com.V8.R6+.tdat available in Geochemist's Workbench format at: https://www.gwb.com/thermo.php. The data produced from these models are available online at (White, 2024).

References

Alanezi, K., & Hilal, N. (2007). Scale formation in desalination plants: effect of carbon dioxide solubility. *Desalination*, *204*, 385–402. https://doi.org/10.1016/j.desal.2006.04.036

de Bergh, C., Moroz, V. I., Taylor, F. W., Crisp, D., Bézard, B., & Zasova, L. V. (2006). The composition of the atmosphere of Venus below 100km altitude: An overview. *Planetary and Space Science*, *54*(13), 1389–1397. https://doi.org/10.1016/j.pss.2006.04.020

Bézard, B., De Bergh, C., Fegley, B., Maillard, J., Crisp, D., Owen, T., et al. (1993). The abundance of sulfur dioxide below the clouds of Venus. *Geophysical Research Letters*, *20*(15), 1587–1590. https://doi.org/10.1029/93GL01338

Chevrier, V. F., & Morisson, M. (2021). Carbonate-Phyllosilicate Parageneses and Environments of Aqueous Alteration in Nili Fossae and Mars. *Journal of Geophysical Research: Planets*, *126*(4). https://doi.org/10.1029/2020JE006698

Donahue, T. M., & Hodges, R. R. (1993). Venus methane and water. *Geophysical Research Letters*, *20*(7), 591–594. https://doi.org/10.1029/93GL00513

Donahue, T. M., & Russell, C. T. (1997). The Venus atmosphere and ionosphere and the interaction with the solar wind: An overview. In S. W. Bougher, D. M. Hunten, & R. J. Phillips (Eds.), Venus II: Geology, geophysics, atmosphere, and solar wind environment (pp. 3). Tucson, AZ: University of Arizona Press

Fegley, B., Zolotov, M. Yu., & Lodders, K. (1997). The Oxidation State of the Lower Atmosphere and Surface of Venus. *Icarus*, *125*(2), 416–439. https://doi.org/10.1006/icar.1996.5628

Filiberto, J., Trang, D., Treiman, A. H., & Gilmore, M. S. (2020). Present-day volcanism on Venus as evidenced from weathering rates of olivine. *Science Advances*, *6*(1), eaax7445. https://doi.org/10.1126/sciadv.aax7445

Gilmore, M. S., Mueller, N., & Helbert, J. (2015). VIRTIS emissivity of Alpha Regio, Venus, with implications for tessera composition. *Icarus*, *254*, 350–361. https://doi.org/10.1016/j.icarus.2015.04.008

Herrick, R. R., & Hensley, S. (2023). Surface changes observed on a Venusian volcano during the Magellan mission. *Science*, *379*(6638), 1205–1208. https://doi.org/10.1126/science.abm7735

Hoffman, J. H., Hodges, R. R., Donahue, T. M., & McElroy, M. B. (1980). Composition of the Venus lower atmosphere from the Pioneer Venus Mass Spectrometer. *Journal of Geophysical Research: Space Physics*, *85*(A13), 7882–7890. https://doi.org/10.1029/JA085iA13p07882

Hoffman, J. H., Oyama, V. I., & von Zahn, U. (1980). Measurements of the Venus lower atmosphere composition: A comparison of results. *Journal of Geophysical Research*, *85*(A13), 7871. https://doi.org/10.1029/JA085iA13p07871

Hu, X., Yao, S., He, M., Ding, Z., Cui, Y., Shen, J., et al. (2014). Geochemistry, U-Pb Geochronology and Hf Isotope Studies of the Daheishan Porphyry Mo Deposit in Heilongjiang Province, NE China: Daheishan porphyry Mo Deposit, NE China. *Resource Geology*, *64*(2), 102–116. https://doi.org/10.1111/rge.12031

Kasting, J. F. (1988). Runaway and moist greenhouse atmospheres and the evolution of Earth and Venus. *Icarus*, *74*(3), 472–494. https://doi.org/10.1016/0019-1035(88)90116-9

Kasting, J. F. (1993). Earth's Early Atmosphere. *Science*, *259*(5097), 920–926.

Kohler, E. (2016). Investigating Mineral Stability under Venus Conditions: A Focus on the Venus Radar Anomalies. *Graduate Theses and Dissertations*. Retrieved from https://scholarworks.uark.edu/etd/1473

Kopparapu, R. K., Ramirez, R., Kasting, J. F., Eymet, V., Robinson, T. D., Mahadevan, S., et al. (2013). HABITABLE ZONES AROUND MAIN-SEQUENCE STARS: NEW ESTIMATES. *The Astrophysical Journal*, *765*(2), 131. https://doi.org/10.1088/0004-637X/765/2/131

Krasnopolsky, V. (2007). Chemical kinetic model for the lower atmosphere of Venus. *Icarus*, *191*(1), 25–37. https://doi.org/10.1016/j.icarus.2007.04.028

Krissansen-Totton, J., Fortney, J. J., & Nimmo, F. (2021). Was Venus Ever Habitable? Constraints from a Coupled Interior–Atmosphere–Redox Evolution Model. *The Planetary Science Journal*, *2*(5), 216. https://doi.org/10.3847/PSJ/ac2580

Mukherjee, D., Ghose, N. C., & Chatterjee, N. (2005). Crystallization history of a massif anorthosite in the eastern Indian shield margin based on borehole lithology. *Journal of Asian Earth Sciences*, *25*(1), 77–94. https://doi.org/10.1016/j.jseaes.2004.01.012

Oyama, V. I., Carle, G. C., Woeller, F., Pollack, J. B., Reynolds, R. T., & Craig, R. A. (1980). Pioneer Venus gas chromatography of the lower atmosphere of Venus. *Journal of Geophysical Research: Space Physics*, *85*(A13), 7891–7902. https://doi.org/10.1029/JA085iA13p07891

Semprich, J., Filiberto, J., & Treiman, A. H. (2020). Venus: A phase equilibria approach to model surface alteration as a function of rock composition, oxygen- and sulfur fugacities. *Icarus*, *346*, 113779. https://doi.org/10.1016/j.icarus.2020.113779

Surkov, Yu. A., Barsukov, V. L., Moskalyeva, L. P., Kharyukova, V. P., & Kemurdzhian, A. L. (1984). New data on the composition, structure, and properties of Venus rock obtained by

Venera 13 and Venera 14. *Journal of Geophysical Research*, *89*(S02), B393. https://doi.org/10.1029/JB089iS02p0B393

Way, M. J., & Del Genio, A. D. (2020). Venusian Habitable Climate Scenarios: Modeling Venus Through Time and Applications to Slowly Rotating Venus-Like Exoplanets. *Journal of Geophysical Research: Planets*, *125*(5). https://doi.org/10.1029/2019JE006276

White, H. T. (2024). Thermodynamic Modeling of Alterations During Climate Transition Reveals Evidence of Past Temperate Conditions on Venus (Version 1), Zenodo [Dataset]. https://doi.org/10.5281/zenodo.10565433

Yung, Y. L., & Demore, W. B. (1982). Photochemistry of the stratosphere of Venus: Implications for atmospheric evolution. *Icarus*, *51*(2), 199–247. https://doi.org/10.1016/0019-1035(82)90080-X

Zheng, H., Yu, T., Qu, C., Li, W., & Wang, Y. (2020). Basic Characteristics and Application Progress of Supercritical Water. *IOP Conference Series: Earth and Environmental Science*, *555*(1), 012036. https://doi.org/10.1088/1755-1315/555/1/012036

Zolotov, M. Yu. (2007). 10.10 - Solid Planet–Atmosphere Interactions. In G. Schubert (Ed.), *Treatise on Geophysics* (pp. 349–369). Amsterdam: Elsevier. https://doi.org/10.1016/B978-044452748-6.00181-4

Zolotov, Mikhail Yu., Fegley, B., & Lodders, K. (1997). Hydrous Silicates and Water on Venus. *Icarus*, *130*(2), 475–494. https://doi.org/10.1006/icar.1997.5838

References from the Supporting Information

Alanezi, K., & Hilal, N. (2007). Scale formation in desalination plants: effect of carbon dioxide solubility. *Desalination*, *204*, 385–402. https://doi.org/10.1016/j.desal.2006.04.036

Armstrong, F. A. J. (1957). The iron content of sea water. *Journal of the Marine Biological Association of the United Kingdom*, *36*(3), 509–517. https://doi.org/10.1017/S0025315400025807

Barsukov, V. L., Volkov, V. P., & Khodakovsky, I. L. (1982). The crust of Venus: Theoretical models of chemical and mineral composition. *Journal of Geophysical Research*, *87*(S01), A3. https://doi.org/10.1029/JB087iS01p000A3

Barsukov, V. L., Surkov, Iu. A., Dmitriev, L. V., & Khodakovskii, I. L. (1986). Geochemical studies of Venus by Vega-1 and Vega-2 landers. *Geokhimiia*, 275–288.

Bethke, C. M. (2021). *Geochemical and Biogeochemical Reaction Modeling* (3rd ed.). Cambridge University Press. https://doi.org/10.1017/9781108807005

Bindschadler, D. L. (1995). Magellan: A new view of Venus' geology and geophysics. *Reviews of Geophysics*, *33*, 459. https://doi.org/10.1029/95RG00281

Chevrier, V. F., & Morisson, M. (2021). Carbonate-Phyllosilicate Parageneses and Environments of Aqueous Alteration in Nili Fossae and Mars. *Journal of Geophysical Research: Planets*, *126*(4). https://doi.org/10.1029/2020JE006698

Debye, Peter & Hückel, Erich (1923). The theory of electrolytes. I. Freezing point depression and related phenomena [*Zur Theorie der Elektrolyte. I. Gefrierpunktserniedrigung und verwandte Erscheinungen*]. *Physikalische Zeitschrift*. 24: 185–206. Translated and typeset by Michael J. Braus (2020).

Gilmore, M. S., Mueller, N., & Helbert, J. (2015). VIRTIS emissivity of Alpha Regio, Venus, with implications for tessera composition. *Icarus*, *254*, 350–361. https://doi.org/10.1016/j.icarus.2015.04.008

Goldblatt, C., Claire, M. W., Lenton, T. M., Matthews, A. J., Watson, A. J., & Zahnle, K. J. (2009). Nitrogen-enhanced greenhouse warming on early Earth. *Nature Geoscience*, *2*(12), 891–896. https://doi.org/10.1038/ngeo692

Hu, X., Yao, S., He, M., Ding, Z., Cui, Y., Shen, J., et al. (2014). Geochemistry, U-Pb Geochronology and Hf Isotope Studies of the Daheishan Porphyry Mo Deposit in Heilongjiang Province, NE China: Daheishan porphyry Mo Deposit, NE China. *Resource Geology*, *64*(2), 102–116. https://doi.org/10.1111/rge.12031

Hydes, D. J. (1977). Dissolved aluminium concentration in sea water. *Nature*, *268*(5616), 136–137. https://doi.org/10.1038/268136a0

Ivanov, M. A., & Head, J. W. (1996). Tessera terrain on Venus: A survey of the global distribution, characteristics, and relation to surrounding units from Magellan data. *Journal of Geophysical Research: Planets*, *101*(E6), 14861–14908. https://doi.org/10.1029/96JE01245

Kasting, J. F. (1993). Earth's Early Atmosphere. *Science*, *259*(5097), 920–926.

Marty, B., Zimmermann, L., Pujol, M., Burgess, R., & Philippot, P. (2013). Nitrogen Isotopic Composition and Density of the Archean Atmosphere. *Science*, *342*(6154), 101–104. https://doi.org/10.1126/science.1240971

McKinnon, W. B., Zahnle, K. J., Ivanov, B. A., & Melosh, H. J. (1997). Cratering on Venus: Models and observations. In Bougher, S. W., Hunten, D. M., & Phillips, R. J. (Eds.), Venus II: Geology, geophysics, atmosphere, and solar wind environment (pp. 969). Tucson, AZ: University of Arizona Press.

Mukherjee, D., Ghose, N. C., & Chatterjee, N. (2005). Crystallization history of a massif anorthosite in the eastern Indian shield margin based on borehole lithology. *Journal of Asian Earth Sciences*, *25*(1), 77–94. https://doi.org/10.1016/j.jseaes.2004.01.012

Sato, T. M., & Sagawa, H. (2023). A new constraint on HCl abundance at the cloud top of Venus. *Icarus*, *390*, 115307. https://doi.org/10.1016/j.icarus.2022.115307

Som, S. M., Catling, D. C., Harnmeijer, J. P., Polivka, P. M., & Buick, R. (2012). Air density 2.7 billion years ago limited to less than twice modern levels by fossil raindrop imprints. *Nature*, *484*(7394), 359–362. https://doi.org/10.1038/nature10890

Surkov, Yu. A., Barsukov, V. L., Moskalyeva, L. P., Kharyukova, V. P., & Kemurdzhian, A. L. (1984). New data on the composition, structure, and properties of Venus rock obtained by Venera 13 and Venera 14. *Journal of Geophysical Research*, *89*(S02), B393. https://doi.org/10.1029/JB089iS02p0B393

Way, M. J., Del Genio, A. D., Kiang, N. Y., Sohl, L. E., Grinspoon, D. H., Aleinov, I., et al. (2016). Was Venus the first habitable world of our solar system? *Geophysical Research Letters*, *43*(16), 8376–8383. https://doi.org/10.1002/2016GL069790

White, H. T. (2024). Thermodynamic Modeling of Alterations During Climate Transition Reveals Evidence of Past Temperate Conditions on Venus (Version 1), Zenodo [Dataset]. https://doi.org/10.5281/zenodo.10565433